UMD-40762-400

Pion Polarizabilities and Volume Effects in Lattice QCD

Jie Hu,[1,*] Fu-Jiun Jiang,[2,†] and Brian C. Tiburzi[1,3,‡]

[1]*Department of Physics, Duke University, Box 90305, Durham, NC 27708-0305, USA*
[2]*Institute for Theoretical Physics, Bern University, Sidlerstrasse 5, CH-3012 Bern, Switzerland*
[3]*Maryland Center for Fundamental Physics, Department of Physics, University of Maryland, College Park, MD 20742-4111, USA*

(Dated: February 1, 2008)

Abstract

We use chiral perturbation theory to study the extraction of pion electromagnetic polarizabilities from lattice QCD. Chiral extrapolation formulae are derived for partially quenched QCD, and quenched QCD simulations. On a torus, volume dependence of electromagnetic observables is complicated by $SO(4)$ breaking, as well as photon zero-mode interactions. We determine finite volume corrections to the Compton scattering tensor of pions. We argue, however, that such results cannot be used to ascertain volume corrections to polarizabilities determined in lattice QCD with background field methods. Connection is lacking because momentum expansions are not permitted in finite volume. Our argument also applies to form factors. Volume effects for electromagnetic moments cannot be deduced from finite volume form factors.

PACS numbers: 12.38.Gc, 12.39.Fe

*hujie@phy.duke.edu
†fjjiang@itp.unibe.ch
‡bctiburz@umd.edu

I. INTRODUCTION

Electromagnetic polarizabilities encode fundamental properties of bound states. The electric polarizability of the ground state hydrogen atom, for example, $\alpha_E^H = \alpha_{fs} N/m_e E_0^2$, represents the ease at which the atomic electron cloud deforms in an applied electric field. Here $\alpha_{fs} = e^2/4\pi$ is the fine structure constant, m_e is the electron mass, E_0 is the ground state energy, and N is a pure number, which turns out to be 9/8. Atomic polarizability data are well described by theoretical calculations using atomic wave-functions of the weakly bound electrons. Hadronic polarizabilities, on the other hand, involve non-perturbative physics. The electrically charged quarks inside hadrons respond to applied electromagnetic fields but against the strong chromo-electromagnetic forces that confine them into bound states. If the pion were a weakly bound system of quarks with mass m_q, we might expect its electric polariazability to be of the form, $\alpha_E^\pi \sim \alpha_{fs} N/m_q m_\pi^2$. The actual behavior is considerably different, $\alpha_E^\pi = \alpha_{fs} N/m_\pi \Lambda_\chi^2$, where Λ_χ is the chiral symmetry breaking scale. It thus appears that the pion cloud of the pion is what deforms in the applied field, and that the relevant energy scale is Λ_χ, which is an order of magnitude greater than the pion mass. Compared to the weakly bound scenario, the electric polarizability is a few orders of magnitude smaller, which indicates stiffness of quarks inside hadrons.

Chiral peturbation theory (χPT) [1] provides a low-energy effective theory of QCD from which the pion polarizabilities can be calculated in terms of a few low-energy constants [2]. At leading order in the chiral power counting, calculated values for the pure number N are $N^{\pi^0} = -1/3$ for the neutral pion, and $N^{\pi^\pm} \approx 1/6$ for the charged pions. Comparing these polarizability predictions to experimental data is unlike the situation with atomic polarizabilities. Without stable targets, experimental determination is considerably challenging at best. Pion polarizabilities, however, have been probed indirectly in several experiments. Three reactions are used: radiative pion-nucleon scattering ($\pi N \to \pi N \gamma$), pion photoproduction in photon nucleus scattering ($\gamma A \to \gamma A \pi$), and pion production seen in electron-positron collisions ($\gamma^* \gamma \to \pi\pi$). Neutral pion polarizabilities have been accessed only by the last reaction by the Crystal Ball Collaboration [3]. The most recent experimental effort has been by MAMI at Mainz [4] in measuring the difference of electric and magnetic polarizabilities of the charged pion through radiative pion-nucleon scattering, and by Compass at CERN [5] to measure charged pion polarizabilities using photoproduction off lead. In the latter experiment, final data are being taken, and soon will be analyzed. After the 12 GeV upgrade, Jefferson Lab has plans to measure pion polarizabilities in the future.

Experiments to determine pion polarizabilities have one feature in common: disagreement with predictions from chiral perturbation theory. Considerable effort has been expended to determine polarizabilities to two-loop order in χPT [6, 7, 8, 9], but discrepancy with experiment remains. Because these experiments are indirect, the challenge is removing the hadronic background to isolate the signal. This is a largely model-dependent process with uncontrolled systematic error. Recent dispersion relation calculations, however, appear consistent with experimental values for the polarizabilities [10, 11]. Thus it remains unclear whether disagreement between theory and experiment has its roots in the experimental analysis, or in the behavior of the chiral expansion.

As a first principles method, lattice QCD [12] can be employed to determine pion polarizabilities. Currently and foreseeably this is itself a considerable challenge, but progress has been made with background field methods [13, 14, 15, 16, 17, 18, 19, 20, 21, 22]. Such calculations suffer a number of systematic errors, such as: quenching or partial quenching,

quenching of sea quark charges, and volume effects. While predictions of physical polarizabilities are not currently possible from lattice QCD alone, forthcoming lattice QCD data on polarizabilities can be used as a diagnostic for χPT. The predictions of χPT can be tested against lattice QCD data. To this end, we perform a one-loop analysis of the quenching and partial quenching effects, as well as the volume dependence of pion Compton scattering. As polarizabilities are the coefficients at second order in an expansion in photon momentum ω, one would naively expect that finite volume corrections to polarizabilities can be determined from momentum expanding the finite volume Compton tensor. We find this is not the case. There are many terms in the finite volume Compton tensor not anticipated by infinite volume gauge invariance. All terms, moreover, are form factors in ωL, where L is the spatial size of the lattice. Because of momentum quantization, these form factors cannot be expanded in ωL. Thus the infinite volume connection between the frequency expansion and the polarizabilities is lost. As polarizabilities are typically calculated in lattice QCD using background field methods, this means we cannot use the finite volume Compton tensor to deduce finite volume corrections to polarizabilities extracted from background field correlation functions. The same problem exists for electromagnetic moments. Their volume effects cannot be deduced from series expanding finite volume electromagnetic form factors about zero momentum transfer.

Our work has the following organization. First in Section II A, we detail our conventions for Compton scattering and the electromagnetic polarizabilities of the pion. In Section II B, we review the low-energy effective theories of QCD, and partially quenched QCD. Quenched QCD is discussed in Appendix A. These theories are then utilized in Section II C to compute the pion electromagnetic polarizabilities in infinite volume. Next in Section III, we consider the modifications to polarizabilities in finite volume. These modifications are complicated by both $SO(4)$ breaking and photon zero-mode interactions. We determine the finite volume modifications to pion Compton scattering. Here we argue, however, that these modifications cannot be straightforwardly utilized to ascertain finite volume effects for background field calculations of polarizabilities in lattice QCD. Section IV summarizes our work, and Appendix B collects the finite volume functions employed in the main text.

II. PION COMPTON SCATTERING

A. Compton Scattering Amplitude

For Compton scattering in infinite volume, the amplitude for a real photon to scatter off a pion can be parametrized as

$$\begin{aligned} T_{\gamma\pi} \;=\; & 2m_\pi \left[\left(-\frac{e^2 Q_\pi^2}{m_\pi} + 4\pi\, \alpha_E\, \omega^2 \right) \boldsymbol{\varepsilon}'^{*} \cdot \boldsymbol{\varepsilon} + 4\pi\, \beta_M\, \omega^2 (\boldsymbol{\varepsilon}'^{*} \times \hat{\boldsymbol{k}}') \cdot (\boldsymbol{\varepsilon} \times \hat{\boldsymbol{k}}) \right] \\ & + \frac{e^2 Q_\pi^2}{2m_\pi^2} \omega^2 (\boldsymbol{\varepsilon}'^{*} \cdot \hat{\boldsymbol{k}})(\boldsymbol{\varepsilon} \cdot \hat{\boldsymbol{k}}')(1 - \cos\theta) + \ldots , \end{aligned} \tag{1}$$

where in the center-of-momentum frame the photon momenta are $k_\mu = (\omega, \omega\hat{\boldsymbol{k}})$ for the initial state, and $k'_\mu = (\omega, \omega\hat{\boldsymbol{k}}')$ for the final state. Terms denoted by $\ldots$ are higher order in the photon energy. The frame-dependent scattering angle θ is given by $\cos\theta = \hat{\boldsymbol{k}}' \cdot \hat{\boldsymbol{k}}$. In the above expression, Q_π is the charge of the pion in units of $e > 0$. In writing the physical amplitude,

we have made use of Coulomb gauge in which the initial and final polarization vectors, ε_μ and ε'^*_ν, satisfy $\varepsilon_0 = \varepsilon'^*_0 = 0$. The Compton amplitude appearing above, moreover, includes the one-particle reducible and irreducible pieces, as we have retained the Born terms.

The frequency independent term proportional to Q_π^2 reproduces the Thomson cross-section for low-energy scattering of charged particles when the amplitude squared is combined with appropriate phase-space factors. This term is exactly fixed by the total charge of the system in accordance with the Gell-Mann–Golberger–Low low energy theorems [23, 24]. The induced E1-E1 interaction strength α_E is the electric polarizability, while the induced M1-M1 interaction strength β_M is the magnetic polarizability. In order to identify these as polarizabilities one must pull out a factor of twice the target mass from the Compton amplitude, as we have in Eq. (1). The electric and magnetic polarizabilities are the first structure dependent terms in the low-energy expansion of the Compton scattering amplitude. These polarizabilities can be determined from first principles using lattice QCD techniques. In order to make the connection between lattice data and real world QCD, extrapolations in quark mass and lattice volume are required. To perform these requisite extrapolations, we turn to the low-energy effective theory of QCD, χPT.

B. PQχPT for Pion Compton Scattering

In current lattice calculations, valence and sea quarks are often treated differently. In the rather extreme approximation known as quenched QCD, the sea quarks are completely absent. Less extreme is partially quenched QCD, where sea quarks are retained but have different masses than their valence counterparts. While both approximations are certainly contrary to nature, the latter retains QCD as a limit. Observables computed in partially quenched QCD can be connected to their real world values by utilizing partially quenched χPT (PQχPT) to derive formulae for the required extrapolation in sea quark mass. Because χPT is contained as a limiting case of PQχPT, we focus our discussion on PQχPT. Peculiarities of quenched χPT (QχPT) will be noted where relevant and the general conventions appear in Appendix A. For further details on QχPT and PQχPT, see [25, 26, 27, 28, 29, 30, 31].

To determine pion observables, we imagine that the strange quark mass is fixed at the physical value so that no extrapolations are needed in the valence strange or sea strange quark masses. To this end, we consider a partially quenched theory of valence u and d quarks, paired with degenerate ghost quarks $\tilde{u}$ and $\tilde{d}$, and two additional sea quarks j and l. The quark masses are given in a matrix

$$m_Q = \mathrm{diag}\left(m_u, m_d, m_j, m_l, m_u, m_d\right), \tag{2}$$

where the last two entries are ghost quark masses that are degenerate with their valence counterparts. For simplicity below, we work in the isospin limit of the valence and sea sectors, so that $m_u = m_d$ and $m_j = m_l$. PQχPT describes the low-energy dynamics of partially quenched QCD and is written in terms of the mesons Φ that appear in the coset field Σ as[1]

$$\Sigma = \exp\left(\frac{2i\Phi}{f}\right). \tag{3}$$

[1] In our conventions, the pion decay constant $f \approx 132\,\mathtt{MeV}$.

These mesons are the pseudo-Goldstone modes appearing from spontaneous chiral symmetry breaking: $SU(4|2)_L \otimes SU(4|2)_R \to SU(4|2)_V$. The dynamics of these modes is described at leading-order by the PQχPT Lagrangian

$$\mathcal{L} = \frac{f^2}{8}\text{str}\left(D_\mu \Sigma^\dagger D^\mu \Sigma\right) + \lambda\frac{f^2}{4}\text{str}\left(m_Q^\dagger \Sigma + \Sigma^\dagger m_Q\right) - m_0^2\Phi_0^2. \tag{4}$$

Here $\Phi_0 = \text{str}(\Phi)/\sqrt{2}$ is the flavor singlet field which has been included as a device to obtain the flavor neutral propagators in PQχPT. Expanding the Lagrangian to tree-level, one finds that mesons composed of a quark Q_i and antiquark $\overline{Q}_j$ have masses given by

$$m_{Q_i Q_j}^2 = \lambda\left[(m_Q)_{ii} + (m_Q)_{jj}\right]. \tag{5}$$

The flavor singlet field additionally acquires a mass m_0^2. In PQχPT (as well as in χPT), the strong $U(1)_A$ anomaly generates a mass for the flavor singlet field and hence m_0 can be taken on the order of the chiral symmetry breaking scale, $m_0 \sim \Lambda_\chi \approx 4\pi f$. The flavor singlet field can thus be integrated out. Flavor neutral propagators in PQχPT, however, cannot be diagonalized into simple single pole forms [31]. This fact notwithstanding, the results of our calculations will not require the explicit form of these flavor neutral propagators.

In writing the above theory of mesons, we have added the effects of electromagnetism in the leading-order Lagrangian. The $U(1)$ gauge field, A_μ, appears in the action of the covariant derivative, D_μ, namely

$$D_\mu \Sigma = \partial_\mu \Sigma + ieA_\mu\left[\mathcal{Q}, \Sigma\right], \tag{6}$$

where $\mathcal{Q}$ is the quark electric charge matrix. To completely specify how electromagnetism is coupled, we must extend the quark charges to the partially quenched theory. The choice

$$\mathcal{Q} = \text{diag}\left(q_u, q_d, q_j, q_l, q_u, q_d\right), \tag{7}$$

with $q_j + q_l \neq 0$, is particularly useful because it retains sensitivity to all electromagnetic couplings in the theory as well as maintains the cancellation of disconnected operator insertions between the valence and ghost sectors [32, 33]. Other choices are possible but can be computationally cumbersome in actual lattice simulations.

C. Pion Polarizabilities in Infinite Volume

To determine the pion polarizabilities, we calculate the Compton scattering amplitude for the process $\gamma\pi \to \gamma\pi$ using PQχPT. Contributions to the amplitude are of three types: tree-level, wavefunction renormalization corrections, and one-loop contributions. The first contributions arise from tree-level graphs generated from local electromagnetic vertices in the effective theory. The relevant diagrams have been depicted in Figure 1, and are only non-vanishing for the charged pion. The first diagram represents the local coupling of two photons to the pion. This diagram arises from both the charge-squared operator contained in the leading-order Lagrangian, as well as from terms in the next-to-leading order Lagrangian. Specifically in the notation of [34], the local two-photon, two-pion interactions are contained in the next-to-leading order terms[2]

$$\mathcal{L} = i\,e\,\alpha_9\,F_{\mu\nu}\,\text{str}\left(\mathcal{Q}D^\mu\Sigma D^\nu\Sigma^\dagger + \mathcal{Q}D^\mu\Sigma^\dagger D^\nu\Sigma\right) + e^2\alpha_{10}\,F^2\text{str}\left(\mathcal{Q}\Sigma\mathcal{Q}\Sigma^\dagger\right), \tag{8}$$

[2] Although we use the $SU(3)$ notation for these terms, final results depend on the scale-independent combination $\alpha_9 + \alpha_{10}$, which has the same value in $SU(2)$ as it does in $SU(3)$.

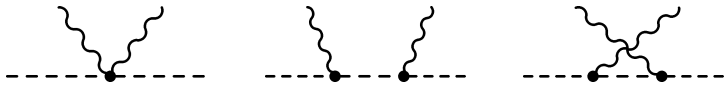

FIG. 1: Tree-level contributions to the Compton scattering amplitude. The dashed lines represent mesons, while the wiggly lines represent photons. Vertices are generated from the leading and next-to-leading order Lagrangian.

FIG. 2: Wavefunction renormalization in PQχPT. Diagram elements are the sames as in Figure 1, and the cross denotes the partially quenched hairpin. The vertex is generated by the leading-order Lagrangian.

where $F_{\mu\nu} = \partial_\mu A_\nu - \partial_\nu A_\mu$ is the electromagnetic field-strength tensor. In PQχPT, the low-energy constants α_9 and α_{10} have the same numerical values as in χPT, which can be demonstrated by matching. The remaining two diagrams in Figure 1 are Born terms that do not contribute to the one-pion irreducible Compton amplitude.

The next contributions are those that arise from the pion wavefunction renormalization. The leading self-energy diagrams are depicted in Figure 2. The leading-order diagrams involving the photon coupling to the pion charge must be multiplied by the wavefunction renormalization to obtain contributions to the Compton amplitude at next-to-leading order. Thus we require only the wavefunction renormalization of the the charged pion. Due to fortuitous cancellation in both PQχPT and QχPT, the hairpin diagram, which arises from the double pole structure of the flavor-neutral propagator, vanishes.

The remaining contributions to the Compton amplitude arise from one-loop diagrams. In Figure 3, we display the diagrams for the one-pion irreducible scattering amplitude. Contributions from such diagrams lead to chiral corrections to the electromagnetic polarizabilities. For the charged pion, there are additional one-pion reducible pieces in PQχPT. These diagrams are displayed in Figure 4. The effects of such diagrams in infinite volume, however, are to renormalize the mass of the intermediate state pion, and to provide the necessary cancellations which preserve the charge interaction of the leading Born terms. The latter cancellations were first worked out explicitly for the case of the pion charge radius in PQχPT in [35, 36]. Assembling the results of Figures 1–4, we can extract the pion polarizabilities using Eq. (1) by utilizing Coulomb gauge in the center-of-momentum frame.

At one-loop order, it is well known that $\alpha_E + \beta_M = 0$ for both charged and neutral pions [2, 37, 38]. We find this remains true to one-loop order in PQχPT, as well as QχPT. This is expected because extending the flavor algebra from $SU(2)$ to graded Lie algebras cannot alter the helicity structure of the Compton amplitude. As for the orthogonal combination of polarizabilities, $\alpha_E - \beta_M$, we arrive at

$$\alpha_E^{\pi^0} - \beta_M^{\pi^0} = -\frac{2\alpha_{fs} Q_\pi^2}{3(4\pi f)^2 m_\pi} \tag{9}$$

$$\alpha_E^{\pi^\pm} - \beta_M^{\pi^\pm} = \frac{16\alpha_{fs} Q_\pi^2 (\alpha_9 + \alpha_{10})}{f^2 m_\pi}, \tag{10}$$

with $Q_\pi = q_u - q_d$. These results are the same in χPT, PQχPT, and QχPT, with the

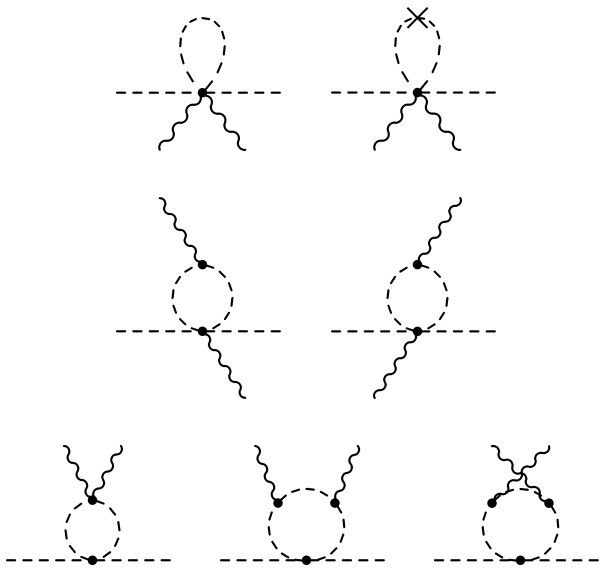

FIG. 3: One-loop contributions to the Compton scattering amplitude in PQχPT. Vertices shown are generated from the leading-order Lagrangian, and diagrams depicted are all one-pion irreducible.

exception that in QχPT the low-energy constants $\alpha_9 + \alpha_{10}$, and f have different numerical values. Furthermore our χPT result agrees with the literature, see [2] (being careful to note $f = \sqrt{2} f_\pi$). In deriving the above result, we remark that the delicate cancellation between pion loops in the zero frequency limit present in χPT remains in PQχPT, and QχPT. This cancellation is required by the infinite volume gauge invariance of the amplitude and reflects that the longest-range coupling to the pion is only to the total charge. In this way the Thomson scattering cross section is produced in these three theories when the zero frequency limit is taken.

In each theory, there are no local electromagnetic interaction terms for the neutral pion in the next-to-leading order Lagrangian. Thus there can be no divergences in the polarizabilities of the neutral pion, as we found explicitly at one-loop. While chiral logarithms are absent for the neutral pion, there are finite terms from the loop graphs. In fact, the entire pion cloud contribution to the neutral pion polarizabilities manages to survive quenching. This is rather surprising, but can be understood by considering the quark-line topologies generated at one-loop order.

The five topologies arising from the four-pion vertex generated from Eq. (4) are depicted in Figure 5. The topologies in the second row are only possible for flavor neutral external states, such as the neutral pion. Let us investigate which topologies can make non-vanishing contributions to the neutral pion polarizabilities. Diagram A contains a sea quark loop and thus associated contributions are proportional to

$$\Delta Q^2 = (q_u - q_j)^2 + (q_u - q_l)^2 + (q_d - q_j)^2 + (q_d - q_l)^2, \tag{11}$$

which sums the charge-squared couplings from all possible valence-sea loop mesons. In the isospin limit of $SU(4|2)$ all such mesons are degenerate with mass m_{ju}. The net contribution from topology A, however, vanishes because contributions from the four-meson vertex with two derivatives exactly cancel contributions from the four-meson vertex with quark mass in-

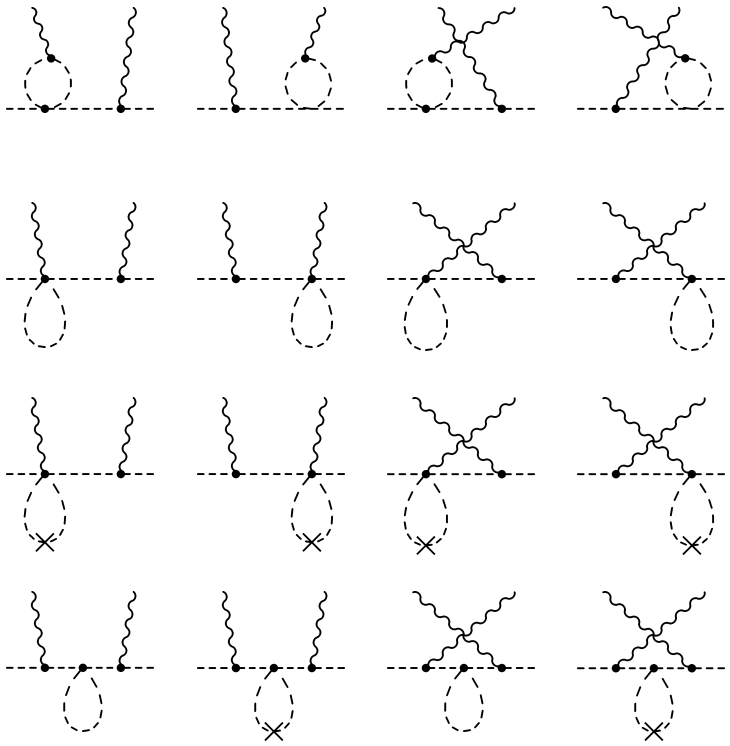

FIG. 4: One-pion reducible contributions to the Compton scattering amplitude at one-loop order in PQχPT.

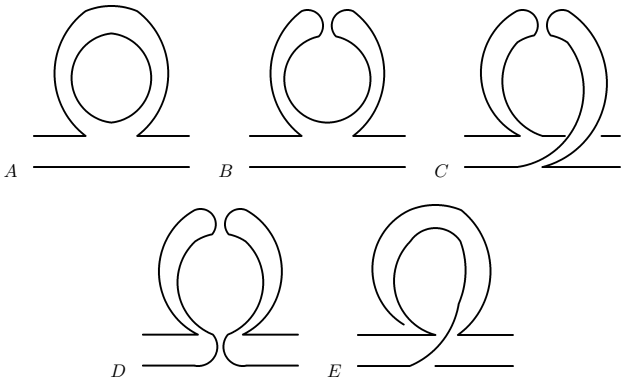

FIG. 5: Quark-line topologies generated at one-loop order. Diagrams in the second row contribute only when the external states are flavor neutral.

sertion. Terms from all of the meson loop diagrams in Figure 3 are required for this delicate cancellation. As a result, the characteristic factor of ΔQ^2 is absent from Eq. (9). Next, each of the quark line topologies B, C, and D, require flavor disconnected contributions from flavor-neutral meson propagators. As flavor neutral mesons are also electrically neutral, coupling to the photon eliminates such contributions. Indeed looking at Figure 3, there is only one possible diagram with a hairpin vertex. Direct evaluation shows that this contribution vanishes, ruling out the B, C, and D topologies. Therefore the loop contributions to

neutral pion polarizabilities in Eq. (9) stem entirely from topology E. As this topology is quark-line connected, the contribution has the same form regardless of quenching.

Let us examine topology E closer by writing the pion field in terms of quark basis mesons, η_u and η_d,

$$\pi^0 = \frac{1}{\sqrt{2}} \left(\eta_n - \eta_d \right). \tag{12}$$

The diagonal contractions, η_u-η_u and η_d-η_d, for topology E result in an electrically neutral loop meson. Only the first diagram of Figure 3 could yield the diagonal contractions of topology E. Close inspection of the Lagrangian shows, however, that the four-meson, two-photon vertex with four electrically neutral mesons is identically zero. Thus neutral pion polarizabilities stem entirely from topology E's non-diagonal flavor contractions: η_u-η_d, and η_d-η_u. To one-loop order, the neutral pion polarizabilities arise entirely from annihilation contractions of lattice QCD correlation functions.

Returning to Eq. (10) for the charged pion polarizabilities, the quark-line picture helps to show why Eq. (10) has no loop contributions. In Figure 5, the quark-line topologies in the second row are no longer relevant because the external states are charged. Furthermore topologies B and C require hairpins, but the hairpin graphs in Figures 2 and 3 vanish. Loop contributions to charged pion polarizabilities can only arise from topology A. Cancellation of divergent loop contributions from this topology must occur in χPT, PQχPT, and QχPT because the combination $\alpha_9 + \alpha_{10}$ is renormalization scale independent. This independence disallows chiral logarithms from loop contributions in χPT, and QχPT. While one can imagine scale invariant combinations of the form $\log(m_{ju}^2/m_{lu}^2)$, say, away from the isopsin limit of $SU(4|2)$, charge-squared couplings do not allow for loop contributions to alternate in sign, see Eq. (11). Thus such logarithms are absent. While logarithms are not allowed, finite contributions can be present. As with the neutral pions for topology A, however, the contributions from the four-meson vertex with two derivatives exactly cancel contributions from the four-meson vertex with quark mass insertion. The characteristic factor of ΔQ^2 is consequently absent from from the charged pion polarizabilities, Eq. (10). Thus the accidental cancellation of finite terms in χPT also occurs in PQχPT, and QχPT.

As a final comment on the inifinite volume results in Eqs. (9) and (10), the only pion mass dependence in both charged and neutral pion polarizabilities arises from the target mass m_π. The target mass depends on the valence quark mass. Both of these statements hold only to one-loop order in the chiral expansion.

III. COMPTON TENSOR IN FINITE VOLUME

In finite volume, the pion is already deformed. Thus its ability to polarize in an applied electric or magnetic field will differ from that in infinite volume. As finite volume modifications to hadron properties are long distance in nature, they can be quite generally addressed using χPT. Lattice simulations are usually carried out in a hypercubic box of volume $L^3 \times \beta$, where L is the length of the spatial direction, and β is the length of the Euclidean time direction. We consider $\beta \gg L$ so that there is no effect from the finite temporal extent of the lattice. With periodic boundary conditions on the quark fields in each of the spatial directions, the momentum modes on the lattice are $\boldsymbol{p} = 2\pi \boldsymbol{n}/L$, with $\boldsymbol{n}$ a triplet of integers. The ordinary power counting for χPT

$$|\boldsymbol{p}| \lesssim m_\pi \ll \Lambda_\chi \tag{13}$$

can be applied in a box of finite size provided $2fL \gg 1$ and $m_\pi L \gtrsim 2\pi$. These two conditions constitute what is called the p-regime of chiral perturbation theory. The first condition is required in order to use chiral perturbation theory at all, while the second condition maintains that pionic zero modes remain perturbative [39, 40]. As the power counting in this regime remains the same as in infinite volume [41], the same diagrams depicted in Figures 1-4 contribute to the pion Compton tensor. It is straightforward to perform the loop calculations in a finite box, we merely replace integrals over virtual four-momenta by integrals over energy and sums over spatial momentum modes permitted by periodicity.

Consider an observable X calculated in both finite and infinite volume. Let $X(L)$ denote the value of the observable in finite volume, and $X(\infty)$ denote its value in infinite volume. The finite and infinite volume theories share exactly the same ultraviolet divergences, thus the volume effect can be determined from matching the two theories in the infrared,

$$X(L) = X(\infty) + \Delta X(L). \tag{14}$$

The volume effect is given by the matching term $\Delta X(L)$ which is ultraviolet finite. A salient feature of such matching is that it allows us to retain our infinite volume regularization scheme and values of low-energy constants.

Calculating the finite volume matching for the Compton scattering amplitude, while straightforward, is quite involved in practice. We first remark that the decomposition of the Compton tensor in Eq. (1) is no longer valid. That decomposition makes use of the center-of-momentum frame. Finite volume results on a torus have only an S_4 cubic subgroup of the infinite volume $SO(4)$ invariance. Results will thus be frame dependent, and hence, to be general, we must not make recourse to a particular frame. Furthermore, as shown in [42], there are more gauge invariant structures allowed on a torus. Thus more terms than shown in Eq. (1) are allowed at second order in the field strength.

A. Neutral Pion

Carrying out the finite volume matching on the neutral pion Compton amplitude without recourse to a particular frame or gauge, we find

$$\begin{aligned}
\Delta T^{\mu\nu}_{\pi^0}(L) \;=\; & \frac{e^2}{f^2}\sum_{\phi}\mathcal{C}^{\pi^0}_{\phi}\Bigg[-\frac{1}{6}g^{\mu\nu}\int_0^1 dx I_{3/2}(x\boldsymbol{r},m_\phi^2-x(1-x)r^2) \\
& +\delta^{\mu 0}\delta^{\nu 0}\Bigg(\frac{1}{3}\int_0^1 dx\int_0^{1-x} dy I_{3/2}(x\boldsymbol{k}+y\boldsymbol{k'},m_\phi^2-xyr^2) \\
& \quad -\frac{1}{4}\int_0^1 dx\int_0^{1-x} dy[(2x-1)\omega+2y\omega'][2x\omega+(2y-1)\omega']I_{5/2}(x\boldsymbol{k}+y\boldsymbol{k'},m_\phi^2-xyr^2)\Bigg) \\
& +\frac{1}{4}\delta^{\mu 0}\delta^{\nu j}\int_0^1 dx\int_0^{1-x} dy[(2x-1)\omega+2y\omega']\Big\{k'^j I_{5/2}(x\boldsymbol{k}+y\boldsymbol{k'},m_\phi^2-xyr^2) \\
& \quad +2I^j_{5/2}(x\boldsymbol{k}+y\boldsymbol{k'},m_\phi^2-xyr^2)\Big\} \\
& +\frac{1}{4}\delta^{\mu i}\delta^{\nu 0}\int_0^1 dx\int_0^{1-x} dy[(2y-1)\omega'+2x\omega]\Big\{k^i I_{5/2}(x\boldsymbol{k}+y\boldsymbol{k'},m_\phi^2-xyr^2) \\
& \quad +2I^i_{5/2}(x\boldsymbol{k}+y\boldsymbol{k'},m_\phi^2-xyr^2)\Big\} \\
& -\frac{1}{4}\delta^{\mu i}\delta^{\nu j}\int_0^1 dx\int_0^{1-x} dy[4I^{ij}_{5/2}(x\boldsymbol{k}+y\boldsymbol{k'},m_\phi^2-xyr^2)+2k^i I^j_{5/2}(x\boldsymbol{k}+y\boldsymbol{k'},m_\phi^2-xyr^2) \\
& \quad +2k'^j I^i_{5/2}(x\boldsymbol{k}+y\boldsymbol{k'},m_\phi^2-xyr^2)+k^i k'^j I_{5/2}(x\boldsymbol{k}+y\boldsymbol{k'},m_\phi^2-xyr^2)]\Bigg]
\end{aligned} \tag{15}$$

Above we have employed $r_\mu = (k-k')_\mu$ for the momentum transfer, with $k_\mu = (\omega, \omega\hat{\boldsymbol{k}})$, and $k'_\mu = (\omega', \omega'\hat{\boldsymbol{k}}')$ for the photon momenta. To derive the above result, we have employed the reality of initial and final state photons, and taken their spatial momenta to be quantized. The finite volume functions $I_\beta(\boldsymbol{\theta}, m^2)$, $I^i_\beta(\boldsymbol{\theta}, m^2)$, and $I^{ij}_\beta(\boldsymbol{\theta}, m^2)$ are defined in Appendix B. The coefficient for contributing loop mesons $\mathcal{C}^{\pi^0}_\phi$ is given by

$$\mathcal{C}^{\pi^0}_\phi = 3Q^2_\pi\left(2m^2_\pi - r^2\right)\delta_{\phi,\pi} - \frac{3}{2}\Delta Q^2 r^2 \delta_{\phi,ju}. \tag{16}$$

While we have only given the PQχPT coefficients, the χPT, and QχPT results can be trivially deduced from Eq. (16). The latter is possible because there are no hairpin contributions. At zero frequency, the finite volume Compton amplitude for the neutral pion is non-vanishing. This is because the Thomson cross-section is not protected from renormalization in finite volume [42].

B. Charged Pion

The charged pion Compton amplitude at finite volume is even more involved than the neutral result as we must determine both reducible and irreducible contributions. To one-

loop order, the result is

$$
\begin{aligned}
\Delta T^{\mu\nu}_{\pi^\pm}(L) \;=\; & -\frac{3e^2\Delta Q^2}{2f^2}r^2\Bigg\{ -\frac{1}{6}g^{\mu\nu}\int_0^1 dx I_{3/2}(x\boldsymbol{r}, m_{ju}^2 - x(1-x)r^2) \\
& +\delta^{\mu 0}\delta^{\nu 0}\int_0^1 dx\int_0^{1-x} dy\Bigg[\frac{1}{3}I_{3/2}(x\boldsymbol{k}+y\boldsymbol{k'}, m_{ju}^2 - xyr^2) \\
& \qquad -\frac{1}{4}[(2x-1)\omega + 2y\omega'][2x\omega + (2y-1)\omega']I_{5/2}(x\boldsymbol{k}+y\boldsymbol{k'}, m_{ju}^2 - xyr^2)\Bigg] \\
& +\frac{1}{4}\delta^{\mu 0}\delta^{\nu j}\int_0^1 dx\int_0^{1-x} dy[(2x-1)\omega + 2y\omega'] \\
& \qquad \times\Big[k'^j I_{5/2}(x\boldsymbol{k}+y\boldsymbol{k'}, m_{ju}^2 - xyr^2) + 2I^j_{5/2}(x\boldsymbol{k}+y\boldsymbol{k'}, m_{ju}^2 - xyr^2)\Big] \\
& +\frac{1}{4}\delta^{\mu i}\delta^{\nu 0}\int_0^1 dx\int_0^{1-x} dy[(2y-1)\omega' + 2x\omega] \\
& \qquad \times\Big[k^i I_{5/2}(x\boldsymbol{k}+y\boldsymbol{k'}, m_{ju}^2 - xyr^2) + 2I^i_{5/2}(x\boldsymbol{k}+y\boldsymbol{k'}, m_{ju}^2 - xyr^2)\Big] \\
& -\frac{1}{4}\delta^{\mu i}\delta^{\nu j}\int_0^1 dx\int_0^{1-x} dy\Big[4I^{ij}_{5/2}(x\boldsymbol{k}+y\boldsymbol{k'}, m_{ju}^2 - xyr^2) + 2k^i I^j_{5/2}(x\boldsymbol{k}+y\boldsymbol{k'}, m_{ju}^2 - xyr^2) \\
& \qquad + 2k'^j I^i_{5/2}(x\boldsymbol{k}+y\boldsymbol{k'}, m_{ju}^2 - xyr^2) + k^i k'^j I_{5/2}(x\boldsymbol{k}+y\boldsymbol{k'}, m_{ju}^2 - xyr^2)\Big]\Bigg\} \\
& -\frac{2e^2Q_\pi^2}{f^2}\left[2g^{\mu\nu} - \frac{(2P+k)^\mu(P+P'+k)^\nu}{(P+k)^2 - m_\pi^2} - \frac{(2P-k')^\nu(P+P'-k')^\mu}{(P-k')^2 - m_\pi^2}\right]I_{1/2}(m_{ju}^2) \\
& -e^2Q_\pi^2\left[\frac{I^\mu(P,P+k)(P+P'+k)^\nu}{(P+k)^2 - m_\pi^2} + \frac{(2P+k)^\mu I^\nu(P+k,P')}{(P+k)^2 - m_\pi^2}\right. \\
& \quad \left. + \frac{I^\mu(P-k',P')(2P-k')^\nu}{(P-k')^2 - m_\pi^2} + \frac{(P+P'-k')^\mu I^\nu(P,P-k')}{(P-k')^2 - m_\pi^2}\right] \\
& +\frac{e^2Q_\pi^2}{f^2}\Bigg[\delta^{\mu 0}\delta^{\nu 0}\int_0^1 dx\Big[2I_{1/2}(x\boldsymbol{k}, m_{ju}^2) + 2I_{1/2}(x\boldsymbol{k'}, m_{ju}^2) \\
& \qquad - x(2x-1)\left(\omega^2 I_{3/2}(x\boldsymbol{k}, m_{ju}^2) + \omega'^2 I_{3/2}(x\boldsymbol{k'}, m_{ju}^2)\right)\Big] \\
& +\delta^{\mu 0}\delta^{\nu j}\int_0^1 dx\ \Big[x\omega' k'^j I_{3/2}(x\boldsymbol{k'}, m_{ju}^2) + 2x\omega' I^j_{3/2}(x\boldsymbol{k'}, m_{ju}^2) + (2x-1)\omega I^j_{3/2}(x\boldsymbol{k}, m_{ju}^2)\Big] \\
& +\delta^{\mu i}\delta^{\nu 0}\int_0^1 dx\ \Big[x\omega k^i I_{3/2}(x\boldsymbol{k}, m_{ju}^2) + 2x\omega I^j_{3/2}(x\boldsymbol{k}, m_{ju}^2) + (2x-1)\omega' I^i_{3/2}(x\boldsymbol{k'}, m_{ju}^2)\Big] \\
& -\delta^{\mu i}\delta^{\nu j}\int_0^1 dx\Big[2I^{ij}_{3/2}(x\boldsymbol{k}, m_{ju}^2) + 2I^{ij}_{3/2}(x\boldsymbol{k'}, m_{ju}^2) \\
& \qquad + k^i I^j_{3/2}(x\boldsymbol{k}, m_{ju}^2) + k'^j I^i_{3/2}(x\boldsymbol{k'}, m_{ju}^2)\Big]\Bigg\}. \qquad (17)
\end{aligned}
$$

In the above result, the initial (final) pion momentum has been denoted by P (P'). We have employed an abbreviation for the finite volume pion-photon vertex function, $I^\mu(P_2, P_1)$,

which arises from the one-pion reducible diagrams and is given by

$$
\begin{aligned}
I^\mu(P_2,P_1) \;=\; & \frac{1}{f^2}\delta^{\mu 0}\Bigg\{(P_2+P_1)^0\Big[\int_0^1 dx I_{1/2}(x\boldsymbol{\Delta},m_{ju}^2-x(1-x)\Delta^2) \\
& \qquad -\frac{1}{2}(\Delta^0)^2\int_0^1 dx\, x(2x-1)I_{3/2}(x\boldsymbol{\Delta},m_{ju}^2-x(1-x)\Delta^2)\Big] \\
& \qquad +\frac{1}{2}\Delta^0\int_0^1 dx(1-2x)(\boldsymbol{P}_2+\boldsymbol{P}_1)\cdot\boldsymbol{I}_{3/2}(x\boldsymbol{\Delta},m_{ju}^2-x(1-x)\Delta^2)\Bigg\} \\
& +\frac{1}{f^2}\delta^{\mu j}\Bigg\{(P_2+P_1)^i\Big[\int_0^1 dx I^{ij}_{3/2}(x\boldsymbol{\Delta},m_{ju}^2-x(1-x)\Delta^2) \\
& \qquad +\frac{1}{2}\Delta^j\int_0^1 dx I^i_{3/2}(x\boldsymbol{\Delta},m_{ju}^2-x(1-x)\Delta^2)\Big] \\
& \qquad +\Delta^0(P_2+P_1)^0\Big[\int_0^1 dx\, x\Big[I^j_{3/2}(x\boldsymbol{\Delta},m_{ju}^2-x(1-x)\Delta^2) \\
& \qquad +\frac{1}{2}\Delta^j\int_0^1 dx I_{3/2}(x\boldsymbol{\Delta},m_{ju}^2-x(1-x)\Delta^2)\Big]\Bigg\},
\end{aligned}
\tag{18}
$$

with $\Delta^\mu=(P_2-P_1)^\mu$. At zero frequency, we recover the results of [42]. Specifically from the one-pion reducible terms, we see that the current is renormalized. This is possible at finite volume because of gauge invariant zero-mode interactions.

C. Discussion of Finite Volume Results

With Eqs. (15) and (17), we have deduced the finite volume modification to the pion Compton scattering tensor. These results show explicitly broken $SO(4)$ invariance as well as additional structures not anticipated by infinite volume gauge invariance. The finite volume modifications can be directly utilized if two-current, two-pion correlation functions are calculated on the lattice. One merely removes the finite volume effects determined above to isolate the infinite volume physics. Such lattice calculations of the Compton tensor are, however, prohibitively expensive time wise, and will not be performed in the foreseeable future. A practical alternative to these calculations is provided by the background field method. In this approach, a classical electromagnetic field is gauged into the QCD action.[3] One then studies the external field dependence of correlation functions to deduce electromagnetic observables. For example, at infinite volume the energy of a neutral pion in a weak external electric field is

$$
E_\pi(\boldsymbol{p}=\boldsymbol{0})=m_\pi-\frac{1}{2}\alpha_E^\pi\boldsymbol{E}^2+\mathcal{O}(\boldsymbol{E}^4). \tag{19}
$$

Thus by measuring the quadratic energy shift in the external field strength $|\boldsymbol{E}|$, one can deduce the electric polarizability. A practical question is then how to deduce volume corrections to polarizabilities determined from background field methods. Given the relation of the infinite volume Compton tensor to the polarizabilities, one might suspect that the

[3] Implementing this method currently suffers the need to quench effects of the background field. In principle, there is no impediment to coupling a suitably weak background field to sea quarks other than time cost.

finite volume Compton tensor in Eqs. (15) and (17) contains the finite volume corrections to the polarizabilities. We argue that the finite volume Compton tensor has no relevance to volume effects in background field methods. At finite volume, there is no longer a discernible relation between polarizabilities and the Compton tensor.

An analysis of finite volume effects for nucleon polarizabilities for background field methods derived from the Compton tensor, however, was presented in [21]. That analysis employed the Breit frame decomposition of the nucleon Compton tensor in Coulomb gauge. Such results surely cannot be utilized for background field calculations because such calculations are typically done in the rest frame. The finite volume modifications derived, moreover, are polluted by subtle effects from the gauge field due to the nature of gauge invariance on a torus. These effects have nothing to do with polarizabilities. For example, in the center-of-momentum frame, where $k^0 = k'^0 = \omega$, we may encounter a term in the amplitude of the form

$$\mathcal{M} = \ldots + \frac{1}{2}\omega^2 \alpha(L)\, \boldsymbol{\varepsilon}'^{*} \cdot \boldsymbol{\varepsilon} + \ldots, \tag{20}$$

and be tempted to conclude that $\alpha(L)$ is a finite volume correction to the electric polarizability. In a general frame, however, this term could stem from any combination of ω^2, ω'^2, and $\omega\omega'$ structures. In infinite volume only the last term is allowed by gauge invariance, specifically by an operator $\propto \boldsymbol{E}^2$ with a coefficient proportional to the electric polarizability. In finite volume, however, the additional structures ω^2 and ω'^2 are allowed. They stem from single-particle effective theory operators of the form

$$\mathcal{L} = \frac{i}{2}\overline{\alpha}(L)\, \boldsymbol{W}^{(-)} \cdot \frac{\partial \boldsymbol{E}}{\partial t}\ \mathrm{tr}(Q^2\Phi^2), \tag{21}$$

for example, where $W_i^{(-)}$ is the negative parity part of the zero-mode Wilson line W_i, given by

$$W_i = \mathcal{P}_{\boldsymbol{0}} \mathcal{W}_i \mathcal{P}_{\boldsymbol{0}}^{\dagger}, \tag{22}$$

with the Wilson line $\mathcal{W}_i$ as

$$\mathcal{W}_i = \exp\left(\frac{ie}{3}\oint dx_i A_i\right), \tag{23}$$

and $\mathcal{P}_{\boldsymbol{0}}$ as the zero-mode projection operator. The operator in Eq. (21) respects C, P, and T, as well as the cubic symmetry of the torus. Furthermore it is gauge invariant because the zero mode has a periodicity constraint under gauge transformations, see [42]. From Eq. (20), we cannot deduce that $\alpha(L)$ is a finite volume correction to the electric polarizability. In general, one must work in an arbitrary frame to disentangle the zero-mode electric coupling in Eq. (21) from the electric polarizability. An analogous situation exists for magnetic interactions, because the operator,

$$\boldsymbol{\nabla} \cdot \left(\boldsymbol{W}^{(-)} \times \boldsymbol{B}\right) \mathrm{tr}(Q^2\Phi^2), \tag{24}$$

for example, is allowed by symmetries.

The frame and gauge dependence notwithstanding, finite volume modifications to polarizabilities were determined in [21] from Taylor series expanding the Compton amplitude in photon frequency. That procedure is also invalid as we now demonstrate. For simplicity, consider the following finite volume difference function, $I_{1/2}(\boldsymbol{k}, m^2)$, where $\boldsymbol{k}$ is an external photon momentum. To determine finite volume corrections to polarizabilities stemming

from this term, we perform a Taylor series expansion in the external momentum and arrive at

$$I_{1/2}(\boldsymbol{k}, m^2) = I_{1/2}(\boldsymbol{0}, m^2) - \frac{1}{2}\boldsymbol{k}^2 m^2 I_{5/2}(\boldsymbol{0}, m^2) + \mathcal{O}(\boldsymbol{k}^4). \tag{25}$$

If we were interested in determining a hypothetical polarizability X entering the amplitude in the form

$$\mathcal{M} = \ldots + \frac{1}{2}\boldsymbol{k}^2 X + \ldots, \tag{26}$$

then we would be tempted to conclude that the finite volume effect $\Delta X(L)$ is given by

$$\Delta X(L) = -m^2 I_{5/2}(\boldsymbol{0}, m^2). \tag{27}$$

Because the external momentum is itself quantized, instead of Eq. (25) we actually have the exact relation

$$I_{1/2}(\boldsymbol{k}, m^2) = I_{1/2}(\boldsymbol{0}, m^2). \tag{28}$$

This follows trivially from re-indexing the summation over loop momentum modes, or from the periodicity of the elliptic-theta function, see Appendix B. Hence the volume effect for our example is actually $\Delta X(L) = 0$. The reason for this discrepancy is a poorly convergent series expansion.[4] Naively the expansion is in $\boldsymbol{k}^2 = 4\pi^2\boldsymbol{n}^2/L^2$, and thus for large enough box size the finite volume effect should be well approximated by the first few terms in the Taylor series. This is not the case. Because higher-order terms have more derivatives, these contributions effectively have more propagators and hence more sensitivity to the infrared. While we would expect the second term in Eq. (25) to be $1/L^2$ suppressed relative to the first term, the asymptotics show that the volume effect is L^2 enhanced

$$\lim_{L\to\infty} m^2 I_{5/2}(\boldsymbol{0}, m^2)/I_{1/2}(\boldsymbol{0}, m^2) = \frac{1}{3}L^2. \tag{29}$$

The series expansion continues in this fashion: all terms are order one. We can see the same effect more directly by expressing the finite volume difference in terms of the elliptic-theta function, namely

$$I_{1/2}(\boldsymbol{k}, m^2) = \frac{1}{\pi^2 L^2}\int_0^\infty d\lambda e^{-m^2L^2/4\lambda}\Big[\vartheta_3(\pi n, e^{-\lambda})\vartheta_3(0, e^{-\lambda})^2 - 1\Big], \tag{30}$$

for the choice $\boldsymbol{k} = (2\pi n/L, 0, 0)$. A series expansion in $\boldsymbol{k}$ is thus effectively the same as expanding in πn.

Returning to Eqs. (15) and (17), we must ascertain whether we can make sense of a series expansion in frequency for the Compton tensor. Terms of the form

$$r^2\int_0^1 dx I_{3/2}(x\boldsymbol{r}, m^2 - x(1-x)r^2), \tag{31}$$

for example, can be plausibly expanded to second order because this requires only evaluation of the finite volume function at $\boldsymbol{r} = 0$. This was the logic employed in [43] to deduce finite

[4] Another difference between Eqs. (25) and (28) is that the order of summation and differentiation has been interchanged. One can easily show, however, that the summation over modes is uniformly convergent by using the Weierstrass M-test.

volume corrections to the nucleon magnetic moment. As $\boldsymbol{r}$ is not continuous, however, one cannot deduce the small momentum behavior of this term from evaluation at $\boldsymbol{r} = 0$, nor can one deduce the small momentum behavior from Taylor series expanding other terms like

$$\int_0^1 dx I_{3/2}(x\boldsymbol{r}, m^2 - x(1-x)r^2), \tag{32}$$

in the Compton tensor, for example. Series expanding in $\boldsymbol{r}L = 2\pi\boldsymbol{n}$ is nonsense no matter the size of the box length L.[5]

At finite volume, one must treat the terms in the amplitude as form factors in ωL. Thus for electromagnetic form factors at finite volume, for example, volume corrections to electromagnetic moments cannot be deduced. Similarly we are unable to use our results for the finite volume modification of the Compton amplitude to deduce corrections to the pion polarizabilities. At second order in the field strength there are a myriad of new terms allowed by the less restrictive symmetries on a torus: cubic invariance and periodic zero-mode gauge invariance. Furthermore a small frequency expansion at finite volume does not make sense for quantized momenta. Said another way, periodic gauge potentials on a torus do not lead to electromagnetic multipole expansions.

IV. SUMMARY

Above we have investigated chiral and volume corrections to pion Compton scattering using χPT, PQχPT, and QχPT. In infinte volume, straightforward calculation of the Compton amplitude allows us to determine charged and neutral pion polarizabilities in these theories. Due to fortuitous cancellation there is no dependence on the sea quark masses, or sea quark charges at one-loop order in the chiral expansion. The Compton tensor itself does not have any quark mass dependence at this order. Consequently the quark mass dependence of the derived polarizabilities stems from a kinematical prefactor of the inverse target mass. As this valence pion mass is relatively inexpensive to dial, the chiral singularity should be discernible from lattice data at light quark masses. Thus as the chiral regime is approached, one can use the lattice as a diagnostic tool to study the chiral behavior of pion polarizabilities. This can be done most easily for the charged pion. Whereas for the neutral pion, we demonstrated that the polarizabilities at one-loop order stem entirely from annihilation contractions which are notoriously difficult to calculate on the lattice.

When accounting for finite volume effects, however, the situation becomes more complicated. Breaking of $SO(4)$ invariance and the nature of gauge invariance on a torus lead to considerably complicated structure for the Compton tensor. Sea quark charge and mass dependence enter in the one-loop finite volume effects. One cannot unambiguously determine the volume effects for the polarizabilities from the Compton tensor because the Taylor series expansion in quantized momentum is poorly convergent. What was in infinte volume a series expansion in $\omega/m_\pi \ll 1$ that lead to the polarizabilities, now is accompanied by an ill-defined expansion in $\omega L \sim 1$ at finite volume. This means that even at low energies, the finite volume Compton amplitude is a form factor in ωL. Consequently connection of our finite volume results to background field lattice calculations is not possible. Similarly

[5] There is a putative improvement in the convergence of the last term due to the integral over the Feynman parameter. The L scaling of terms in the expansion, however, is unchanged.

finite volume corrections to electromagnetic moments cannot be deduced from momentum expanding finite volume form factors. Further investigation is required to determine volume corrections relevant for observables determined with background field methods.

Acknowledgments

We thank W. Detmold, T. Mehen, and A. Walker-Loud for various discussions. This work is supported in part by the U.S. Dept. of Energy, Grant Nos. DE-FG02-05ER-41368-0 (J.H. and B.C.T.), DE-FG02-93ER-40762 (B.C.T), and by the Schweizerischer Nationalfonds (F.-J.J.).

APPENDIX A: QUENCHED χPT

Here we give the relevant details needed in the calculation of quenched pion polarizabilities. In quenched QCD, contributions from sea quarks are completely neglected. In a quenched theory of two flavors u and d, we additionally have two ghost quarks $\tilde{u}$ and $\tilde{d}$. The mass matrix is now

$$m_Q = \mathrm{diag}\left(m_u, m_d, m_u, m_d\right), \tag{A1}$$

where the final two entries are the masses of the ghost quarks. These equal mass ghost quarks are necessitated so that path integral determinants for the valence quarks are exactly canceled by those from the ghosts. The symmetry breaking pattern in QχPT schematically takes the form $U(2|2)_L \otimes U(2|2)_R \to U(2|2)_V$ because there is no axial anomaly in quenched QCD. The coset field Σ is hence a $U(2|2)$ matrix and the singlet component cannot be integrated out. The dynamics of the pseudo-Goldstone modes is described at leading-order by the QχPT Lagrangian

$$\mathcal{L} = \frac{f^2}{8}\mathrm{str}\left(D_\mu \Sigma^\dagger D^\mu \Sigma\right) + \lambda\frac{f^2}{4}\mathrm{str}\left(m_Q^\dagger \Sigma + \Sigma^\dagger m_Q\right) + \alpha_\Phi D_\mu \Phi_0 D^\mu \Phi_0 - m_0^2 \Phi_0^2. \tag{A2}$$

While propagators for flavor-neutral mesons have double poles, these are not encountered explicitly in expressions for the pion polarizabilities at next-to-leading order. Quenched observables are in general unrelated to their unquenched counterparts, for example, the constants α_Φ and m_0 have no analogs in χPT, moreover, arbitrary polynomial functions of Φ_0^2 can multiply any term in the Lagrangian and the low-energy constants in the quenched chiral Lagrangian above result from treating these polynomial terms in mean-field approximation.

For the quenched electric charge matrix of the quarks, we must have

$$\mathcal{Q} = \mathrm{diag}\left(q_u, q_d, q_u, q_d\right), \tag{A3}$$

for which the condition $\mathrm{str}\mathcal{Q} = 0$ is unavoidable. In general there are fewer local electromagnetic terms in QχPT as compared to χPT. At next-to-leading order, however, both the α_9 and α_{10} terms remain. We must keep in mind that the numerical values of these coefficients are unrelated to their values in χPT. Calculation of the pion polarizabilities then proceeds analogously to the partially quenched case. Results for the quenched polarizabilities have been given for infinite and finite volume in the main text.

APPENDIX B: FINITE VOLUME FUNCTIONS

Above we have determined the finite volume modification to the Compton scattering tensor. In this Appendix, we give explicit formulae for the finite volume functions used to express finite volume differences. We use similar notation for these functions as [44, 45], where further discussion can be found.

In evaluating a Feynman diagram in finite volume, the loop integral is converted into a sum over the allowed Fourier modes in a periodic box. The difference of this sum and the infinite volume result is the finite volume effect. As is customary, we treat the length of the time direction as infinite. All finite volume differences with momentum insertion can be cast in terms of the function $I_\beta^{i_1\cdots i_j}(\boldsymbol{\theta}, m^2)$, defined by

$$I_\beta^{i_1\cdots i_j}(\boldsymbol{\theta}, m^2) = \frac{1}{L^3}\sum_{\boldsymbol{n}} \frac{q^{i_1}\cdots q^{i_j}}{[(\boldsymbol{q}+\boldsymbol{\theta})^2+m^2]^\beta} - \int \frac{d\boldsymbol{q}}{(2\pi)^3}\frac{q^{i_1}\cdots q^{i_j}}{[(\boldsymbol{q}+\boldsymbol{\theta})^2+m^2]^\beta}, \tag{B1}$$

where the sum on $\boldsymbol{n}$ is over triplets of integers, and the loop momentum modes are quantized as $\boldsymbol{q} = 2\pi\boldsymbol{n}/L$ in a periodic box. While a general expression for the exponentially convergent form of $I_\beta^{i_1\cdots i_j}(\boldsymbol{\theta}, m^2)$ exists, it is easiest merely to cite the required cases for our work. These are

$$I_\beta(\boldsymbol{\theta}, m^2) = \frac{(L^2/4)^{\beta-3/2}}{(4\pi)^{3/2}\Gamma(\beta)}\int_0^\infty d\lambda\, \lambda^{1/2-\beta} e^{-m^2L^2/4\lambda}\left[\prod_{j=1}^3 \vartheta_3(\theta_j L/2, e^{-\lambda}) - 1\right] \tag{B2}$$

$$I_\beta^{i_1}(\boldsymbol{\theta}, m^2) = -\frac{1}{2(\beta-1)}\frac{d}{d\theta^{i_1}} I_\beta(\boldsymbol{\theta}, m^2) - \theta^{i_1} I_\beta(\boldsymbol{\theta}, m^2) \tag{B3}$$

$$\begin{aligned} I_\beta^{i_1 i_2}(\boldsymbol{\theta}, m^2) = {} & \frac{1}{4(\beta-2)(\beta-1)}\frac{d^2}{d\theta^{i_1}d\theta^{i_2}} I_{\beta-2}(\boldsymbol{\theta}, m^2) + \frac{1}{2(\beta-1)}\delta^{i_1 i_2} I_{\beta-1}(\boldsymbol{\theta}, m^2) \\ & - \theta^{i_1} I_\beta^{i_2}(\boldsymbol{\theta}, m^2) - \theta^{i_2} I_\beta^{i_1}(\boldsymbol{\theta}, m^2) - \theta^{i_1}\theta^{i_2} I_\beta(\boldsymbol{\theta}, m^2) \end{aligned} \tag{B4}$$

where $\vartheta_3(z, q)$ is a Jacobi elliptic-theta function of the third kind, see, e.g. [46].

[1] J. Gasser and H. Leutwyler, Ann. Phys. **158**, 142 (1984).
[2] B. R. Holstein, Comments Nucl. Part. Phys. **A19**, 221 (1990).
[3] H. Marsiske et al. (Crystal Ball), Phys. Rev. **D41**, 3324 (1990).
[4] J. Ahrens et al., Eur. Phys. J. **A23**, 113 (2005), nucl-ex/0407011.
[5] M. Colantoni (COMPASS), Czech. J. Phys. **55**, A43 (2005).
[6] U. Burgi, Phys. Lett. **B377**, 147 (1996), hep-ph/9602421.
[7] U. Burgi, Nucl. Phys. **B479**, 392 (1996), hep-ph/9602429.
[8] J. Gasser, M. A. Ivanov, and M. E. Sainio, Nucl. Phys. **B728**, 31 (2005), hep-ph/0506265.
[9] J. Gasser, M. A. Ivanov, and M. E. Sainio, Nucl. Phys. **B745**, 84 (2006), hep-ph/0602234.
[10] L. V. Fil'kov and V. L. Kashevarov, Phys. Rev. **C72**, 035211 (2005), nucl-th/0505058.
[11] L. V. Fil'kov and V. L. Kashevarov, Phys. Rev. **C73**, 035210 (2006), nucl-th/0512047.
[12] T. DeGrand and C. DeTar, *Lattice Methods for Quantum Chromodynamics* (World Scientific, 2006).
[13] F. Fucito, G. Parisi, and S. Petrarca, Phys. Lett. **B115**, 148 (1982).

[14] G. Martinelli, G. Parisi, R. Petronzio, and F. Rapuano, Phys. Lett. **B116**, 434 (1982).
[15] C. W. Bernard, T. Draper, K. Olynyk, and M. Rushton, Phys. Rev. Lett. **49**, 1076 (1982).
[16] H. R. Fiebig, W. Wilcox, and R. M. Woloshyn, Nucl. Phys. **B324**, 47 (1989).
[17] M. Burkardt, D. B. Leinweber, and X.-M. Jin, Phys. Lett. **B385**, 52 (1996), hep-ph/9604450.
[18] J. Christensen, W. Wilcox, F. X. Lee, and L.-M. Zhou, Phys. Rev. **D72**, 034503 (2005), hep-lat/0408024.
[19] W. Detmold, Phys. Rev. **D71**, 054506 (2005), hep-lat/0410011.
[20] F. X. Lee, L.-M. Zhou, W. Wilcox, and J. Christensen, Phys. Rev. **D73**, 034503 (2006), hep-lat/0509065.
[21] W. Detmold, B. C. Tiburzi, and A. Walker-Loud, Phys. Rev. **D73**, 114505 (2006), hep-lat/0603026.
[22] M. Engelhardt (LHPC) (2007), arXiv:0706.3919 [hep-lat].
[23] M. Gell-Mann and M. L. Goldberger, Phys. Rev. **96**, 1433 (1954).
[24] F. E. Low, Phys. Rev. **96**, 1428 (1954).
[25] A. Morel, J. Phys. (France) **48**, 1111 (1987).
[26] S. R. Sharpe, Phys. Rev. **D46**, 3146 (1992), hep-lat/9205020.
[27] C. W. Bernard and M. F. L. Golterman, Phys. Rev. **D46**, 853 (1992), hep-lat/9204007.
[28] S. R. Sharpe, Phys. Rev. **D56**, 7052 (1997), hep-lat/9707018.
[29] M. F. L. Golterman and K.-C. Leung, Phys. Rev. **D57**, 5703 (1998), hep-lat/9711033.
[30] S. R. Sharpe and N. Shoresh, Phys. Rev. **D62**, 094503 (2000), hep-lat/0006017.
[31] S. R. Sharpe and N. Shoresh, Phys. Rev. **D64**, 114510 (2001), hep-lat/0108003.
[32] B. C. Tiburzi, Phys. Rev. **D71**, 054504 (2005), hep-lat/0412025.
[33] W. Detmold and C. J. D. Lin, Phys. Rev. **D71**, 054510 (2005), hep-lat/0501007.
[34] J. F. Donoghue, E. Golowich, and B. R. Holstein, Cambridge Monogr. Part. Phys. Nucl. Phys. Cosmol. **2**, 1 (1992).
[35] D. Arndt and B. C. Tiburzi, Phys. Rev. **D68**, 094501 (2003), hep-lat/0307003.
[36] T. B. Bunton, F. J. Jiang, and B. C. Tiburzi, Phys. Rev. **D74**, 034514 (2006), hep-lat/0607001.
[37] J. Bijnens and F. Cornet, Nucl. Phys. **B296**, 557 (1988).
[38] J. F. Donoghue, B. R. Holstein, and Y. C. Lin, Phys. Rev. **D37**, 2423 (1988).
[39] J. Gasser and H. Leutwyler, Phys. Lett. **B184**, 83 (1987).
[40] J. Gasser and H. Leutwyler, Phys. Lett. **B188**, 477 (1987).
[41] J. Gasser and H. Leutwyler, Nucl. Phys. **B307**, 763 (1988).
[42] J. Hu, F.-J. Jiang, and B. C. Tiburzi, Phys. Lett. **B653**, 350 (2007), arXiv:0706.3408 [hep-lat].
[43] S. R. Beane, Phys. Rev. **D70**, 034507 (2004), hep-lat/0403015.
[44] C. T. Sachrajda and G. Villadoro, Phys. Lett. **B609**, 73 (2005), hep-lat/0411033.
[45] B. C. Tiburzi, Phys. Lett. **B641**, 342 (2006), hep-lat/0607019.
[46] J. Zinn-Justin, Int. Ser. Monogr. Phys. **92**, 1 (1996).